Available online at www.sciencedirect.com
SCIENCE DIRECT®
Polymer 44 (2003) 6159–6167
polymer
www.elsevier.com/locate/polymer

Gradient structure materials from homogeneous system induced by UV photopolymerization

N. Désilles, L. Lecamp, P. Lebaudy, C. Bunel*

UMR CNRS 6522 Polymères, Biopolymères, Membranes. Laboratoire de Matériaux Macromoléculaires, Institut National des Sciences Appliquées de Rouen, Place E. Blondel, BP 08, 76131 Mont Saint Aignan Cédex, France

Received 19 March 2003; received in revised form 11 July 2003; accepted 18 July 2003

Abstract

This work deals with the synthesis of a gradient structure material from a homogeneous system of monomers. This new synthesis involved hydroxyethylmethacrylate, a hydroxytelechelic polybutadiene, and 4,4′-methylene-bis(cyclohexylisocyanate). These materials were made in two steps. The first one consisted in creating a photopolymerization gradient in methacrylic double bonds under UV exposure thanks to the decay of UV light intensity through the sample thickness. The second one involved a thermal crosslinking reaction leading to the formation of a polyurethane network in order to set the obtained gradient. Using FTIR and UV spectroscopies, the required experimental conditions to obtain and keep the gradient were investigated. Thus, these parameters enabled us to obtain a 20% hydroxyethylmethacrylate double bonds conversion gradient in the ultimate 5 mm thick material. Further DMA analysis well revealed a difference of structures between the two sides of the material.

Keywords: Gradient structure material; Photopolymerization; Methacrylate network

1. Introduction

Multicomponent polymer systems exhibiting a composition or a structure that varies continuously with the position in the sample have given rise to a great interest in the last years [1–4]. The so-called gradient polymers are mixtures of crosslinked polymers in which the concentration of one of the networks varies across the section of the material [5]. Thus, they can be defined as a combination of an infinite number of layers, each one being a full system with its own composition and properties [6]. The main advantage of such gradient polymers is their possibility, due to their spatial gradient, of making polymer systems with customized properties for different applications [3,7–12].

Several methods suitable to obtain a gradient polymer can be encountered in literature. Thus, two authors have synthesized a GRIN (GRadient INdex) polymer by an interfacial gel copolymerization technique. The gradient was created using two monomers with different refractive index and satisfying the conditions on the reactivity ratios $r_1 > 1$ and $r_2 < 1$ [13,14]. Another way was described by Agari and col. [15] and consists in carrying out the dissolution–diffusion method: a poly(methylmethacrylate) solution was poured onto a poly(vinylchloride) film, thus enabling the dissolution and diffusion of the PVC in the PMMA solution to proceed until evaporation of the solvent is completed. The gradient aforementioned depends on the dissolution and diffusion kinetics of the PVC in the PMMA solution and on the evaporation kinetic of the solvent. Dioxygene too can create a gradient in the area near the surface, through an inhibition reaction of the radical polymerization of styrene in a poly(hydroxyethyl methacrylate) matrix [16].

But the more usual way to obtain a gradient polymer is the sequential curing [17–20]. This largely described method has proved to be useful in the fields of GRIN [21,22] and biomaterials [23,24]. This method takes place in two steps. The first one consists in curing one network, followed by its swelling in components forming the second network. The gradient is obtained by preventing the swelling from reaching its equilibrium value. In the second step, this gradient in concentration of the second network components undergoes ultimately a curing by

* Corresponding author. Tel./fax: +33-2-35-52-84-46.
E-mail address: claude.bunel@insa-rouen.fr (C. Bunel).

0032-3861/$ - see front matter © 2003 Elsevier Ltd. All rights reserved.
doi:10.1016/S0032-3861(03)00664-5

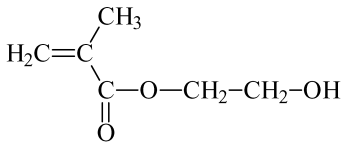

HEMA

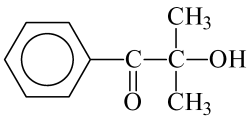

Darocur 1173

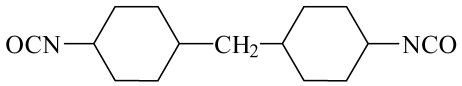

$H_{12}MDI$

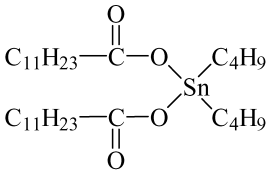

DBTL

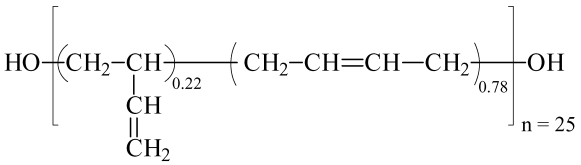

HTPB

Fig. 1. Chemical formula of the reactants used.

photopolymerization [25,26]. Furthermore, the analysis of the monomer diffusion in the matrix is required to predict the gradient structure [27], and problems involved in the effects of various factors influencing the monomer diffusion rate can raise [28].

In works above mentioned, gradient materials were usually all realized from a mixture containing at least one polymer. The present work deals with a new synthesis of gradient materials involving a photopolymerization reaction from a homogeneous system, that is to say a system of monomers. Two steps are envisaged to make these materials. In the first one, a polymerization gradient is photochemically created and obtained thanks to the variation of UV absorbance in the medium. The second step consists in setting the obtained gradient by a thermal crosslinking reaction. With this aim in view, the UV step will make use of hydroxyethylmethacrylate, well known to react radically under UV exposure thanks to its double bonds, and provided with chemical functions able to react thermally with another monomer in the second step, namely hydroxyl groups. Concerning the thermal step, a polyurethane network will be formed using a multifunctional hydroxy oligomer (hydroxy telechelic polybutadiene), a diisocyanate (4,4′-methylene-bis(cyclohexylisocyanate)), and the aforementioned hydroxymethacrylate.

First of all, the required experimental conditions to obtain a gradient by UV irradiation will be determined. Then, the polyurethane formation parameters enabling this gradient to be kept will be set. Finally, the formation kinetics of the material will be investigated.

2. Experimental

2.1. Materials

Fig. 1 shows the chemical formula of the reactants used. Polybutadiene (Poly Bd R20LM®—HTPB) and 4,4′-methylene-bis(cyclohexylisocyanate) ($H_{12}MDI$) were kindly supplied respectively by Atofina and Bayer. HTPB is a low molar mass polybutadiene ($\bar{M}_n = 1370$ g mol^{-1}) and presents an average hydroxy functionality $\bar{f}_{OH} = 2.45$. Microstructure studies indicate 22% of 1,2 units (vinyl units) and 78% of 1,4 units [29]. $H_{12}MDI$ and hydroxyethylmethacrylate (HEMA) (Aldrich) were used as received. Dibutyl tin dilaurate (DBTL) (Aldrich) and 2,2-dimethyl-2-hydroxyacetophenone (Darocur 1173) (Ciba Geigy) were used without further purification.

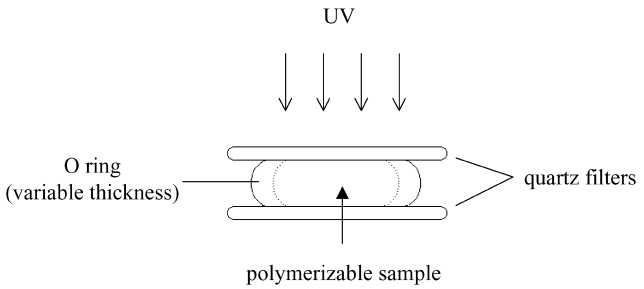

Scheme 1. Schematic shape of the experimental device.

2.2. Preparation of samples

30 mmol (41.1 g) of HTPB were introduced into a 250 ml round bottom flask equipped with a mechanical stirrer (300 rpm), a switchable inlet for nitrogen and a vacuum connector. HTPB was first degassed for 1 h by a graduated vacuum up to 10^{-1}–10^{-2} mm Hg at 80 °C in order to eliminate all volatile products. Then the reactor was placed at room temperature under nitrogen. 78.4 mmol (10.2 g) of HEMA containing 0.15% (w/w) of Darocur 1173 (i.e. 10^{-2} mol l^{-1} compared to the methacrylate monomer) and 76 mmol (19.9 g) of H_{12}MDI were added and the mixture was stirred for 20 min. This mixture was stored at −18 °C until its use. Catalyst (DBTL) (2.4 mmol l^{-1}) was finally introduced carefully as rapidly as possible and just before the use of the reactional mixture returned to room temperature.

Mixture was then run in a mould of various thickness (from 1 to 5 mm) as described in Scheme 1. A quartz filter was deposed on the top of the sample to avoid the inhibitor effect of oxygen. UV radiation is applied 6 min after introduction of the DBTL catalyst in the reactional mixture.

When reaction was studied on film, no O ring was used and the quartz filter was directly deposed on sample.

2.3. Photopolymerization conditions

The UV radiation comes from a 350 W Oriel mercury vapour lamp. Its intensity is measured at the sample level by using a spectroradiometer (Intraspec II Oriel) of which probes are centred on 254, 312 or 365 nm. The radiation is monochromatic by means of the use of interferential filters (254, 289, 312, 334 or 365 nm).

2.4. Thermal crosslinking conditions

Sample unit as described in Scheme 1 is placed in a oven at a given temperature and crosslinking was allowed to proceed until complete disappearance of isocyanate functions.

2.5. Measurements

2.5.1. Real time infrared spectroscopy (RTIR)

Photochemical and thermal polymerization reactions were followed by real time infrared spectroscopy (Perkin–Elmer FTIR 2000 spectrometer) in attenuated total reflection (ATR). In case of films, a sample drop was deposited and spread out over the ATR diamond crystal with a quartz filter. This diamond crystal can be carried at a chosen temperature by a thermocouple. In case of thick materials, samples were realized as shown in Scheme 1, the diamond crystal constituting the lower face of these samples. UV radiation from a 350 W Oriel mercury vapour lamp was introduced into the FTIR spectrometer sample chamber by a flexible light guide so that it did not interfere with the IR beam. The monochromatic UV radiation intensity was usually 6.5 mW/cm^2 at the sample level at 312 nm.

The disappearance of the C=C stretching vibrations of the methacrylate functional groups at 815 and 1638 cm^{-1}, the vinyl C=C stretching vibrations of the HTPB at 910 and 1638 cm^{-1} and the isocyanate band at 2257 cm^{-1} were observed. A reference band in the spectrum was used at 2924 cm^{-1} to calculate conversions. After correction of the baseline, conversion of the methacrylic double bonds and of the isocyanate groups can be calculated by measuring the absorbance at each time of the reaction and determined as following:

$$\chi_{\text{C=C HEMA}_{(t)}} = \frac{\dfrac{A_0^{815}}{A_0^{2924}} - \dfrac{A_t^{815}}{A_t^{2924}}}{\dfrac{A_0^{815}}{A_0^{2924}}} \times 100$$

$$\chi_{\text{NCO}_{(t)}} = \frac{\dfrac{A_0^{2257}}{A_0^{2924}} - \dfrac{A_t^{2257}}{A_t^{2924}}}{\dfrac{A_0^{2257}}{A_0^{2924}}} \times 100$$

where $\chi_{(t)}$ is the conversion of these reactive functions at t time, A_0 is the initial absorbance (before UV irradiation) and A_t is the absorbance of the functional groups at t time.

In the same way, conversion in HTPB vinyl double bonds can be deduced from global conversion in double bonds (methacrylic and vinyl) at 1638 cm^{-1} as follows:

$$A_{\text{HTPB}} = A_{1638} - A_{\text{HEMA}} = A_{1638} - \varepsilon_{\text{HEMA}}^{1638} \ell C_{\text{HEMA}}$$

then

$$\chi_{\text{C=C HTPB}_{(t)}} = \frac{\left(\dfrac{A_0^{1638} - \varepsilon_{\text{HEMA}}^{1638}\ell[\text{HEMA}]_0}{A_0^{2924}}\right) - \left(\dfrac{A_t^{1638} - \varepsilon_{\text{HEMA}}^{1638}\ell[\text{HEMA}]_t^{815}}{A_t^{2924}}\right)}{\dfrac{A_0^{1638} - \varepsilon_{\text{HEMA}}^{1638}\ell[\text{HEMA}]_0}{A_0^{2924}}} \times 100$$

with $\varepsilon_{\text{HEMA}}^{1638}\ell = 1.34 \times 10^{-2}$ mol^{-1} l, $[\text{HEMA}]_0 = 8.25$

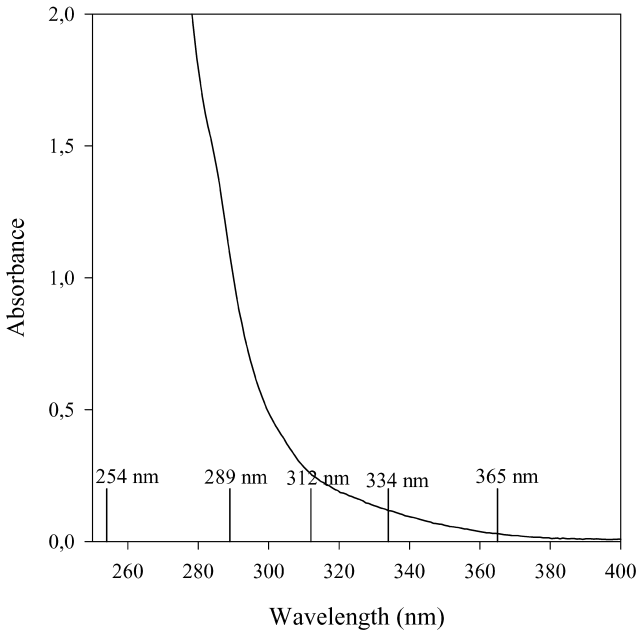

Fig. 2. Absorption spectrum in bulk of reactive mixture and main Hg lamp emission wavelengths.

mol l^{-1} and $[HEMA]_t^{815}$ is the concentration in HEMA at t time determined from the absorbance of the peak at 815 cm^{-1}.

2.5.2. Ultraviolet spectroscopy

Spectral absorbance of the reactive mixture was measured in mass, in quartz cell of 1 mm thickness, by using an UV–Visible spectrophotometer (Perkin–Elmer Lambda 16).

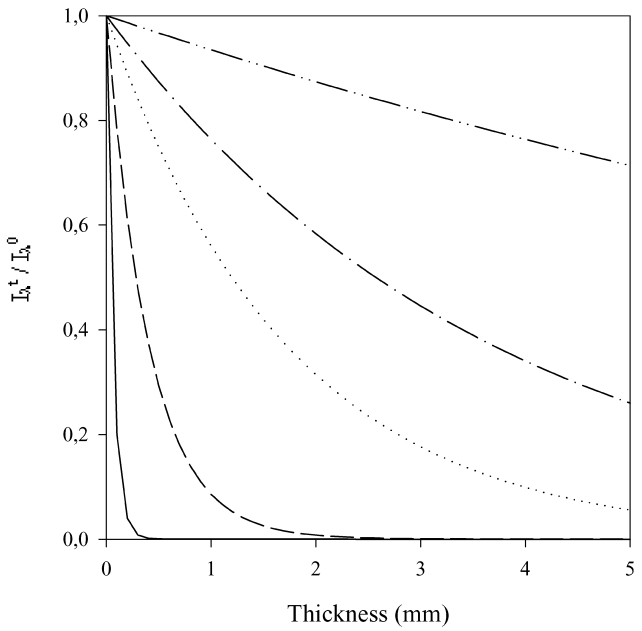

Fig. 3. Absorption of reactive mixture versus thickness at several wavelengths (■ 254 nm, – – – 289 nm, ⋯ 312 nm, –· 334 nm, –·· 365 nm).

2.5.3. Dynamic mechanical analysis (DMA)

Samples were analyzed by dynamic mechanical analysis (DMA 7 Perkin–Elmer) in compression mode with stainless steel parallel plate probe (1 mm diameter), at 1 Hz frequency and 10 °C/min heating rate. The static and dynamic forces applied were respectively 220 and 200 mN. The evolution of tan δ was followed versus temperature.

3. Results and discussion

3.1. Creation of the gradient under UV exposure

The UV induced photopolymerization is a widely used technique in polymer synthesis. However, it should be stressed that a heterogeneous reaction can take place in the medium due to the decay of light intensity through the material thickness. This characteristic of photopolymerization, experienced as a drawback by Murayama and col. [16], is the key to create a polymerization gradient. Indeed, thanks to the sample absorbance and the distribution of light intensity through the irradiated system predicted by Beer–Lambert's law, an intensity gradient, and consequently a polymerization gradient, can be created inside the sample when exposed to UV radiation.

The absorption spectrum of reactive mixture is presented in Fig. 2. One can notice that on the one hand, the reactive mixture shows an absorbance near to zero at 400 nm, and on the other hand, an absorbance superior to 2 when the wavelength is below 280 nm. Therefore, irradiating at 400 nm or higher would be useless and result in no gradient formation. In the same way, choosing 280 nm or downer would only cure the very surface of the material.

According to Beer–Lambert's law:

$$A_\lambda = \log \frac{I_\lambda^0}{I_\lambda^t} = \varepsilon_\lambda l C$$

then

$$\frac{I_\lambda^t}{I_\lambda^0} = 10^{-\varepsilon_\lambda l C}$$

where A_λ is the absorbance at the selected wavelength, I_λ^0 is the incident light intensity, I_λ^t is the transmitted light intensity, ε_λ is the molar extinction coefficient, l is the optical path, C is the concentration of the studied component.

Knowing A_λ from 250 to 400 nm for a 1 mm optical path thanks to Fig. 2, ratios I_λ^t/I_λ^0 for an optical path varying from 0 to 5 mm were plotted in Fig. 3 for the main emission wavelengths of the Hg lamp located at 254, 289, 312, 334 and 365 nm.

These results clearly demonstrate that 254 and 365 nm are not suitable wavelengths to obtain a gradient, whatever

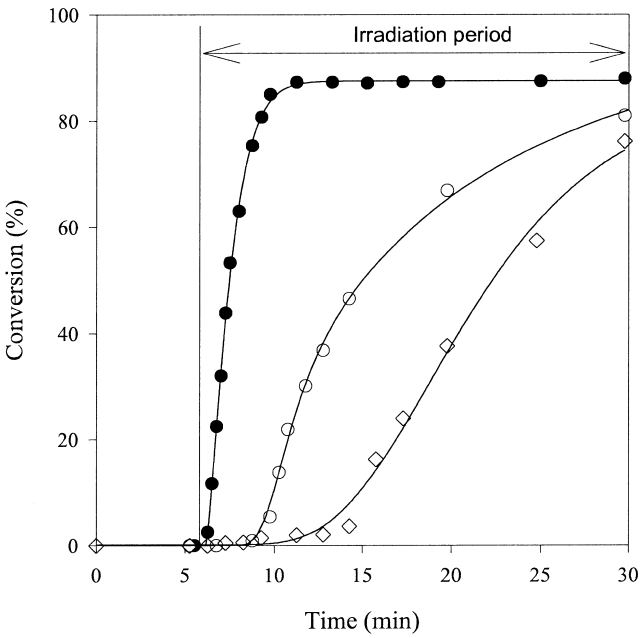

Fig. 4. Conversion of HEMA double bonds versus irradiation time at 30 °C at the surface for 6.5 mW/cm^2 (●), at 5 mm for 6.5 mW/cm^2 (○), and at the surface for 0.36 mW/cm^2 (◇).

the thickness may vary from 0 to 5 mm. The 312 nm wavelength shows a progressive decay of light intensity down to nearby 0 inside the sample, combined with a reasonable 5 mm thickness. Consequently, the irradiation wavelength was set to 312 nm, and the material thickness to 5 mm.

A kinetic study monitored by FTIR was performed on a 5 mm thick sample with a monochromatic UV light intensity of 6.5 mW/cm^2 at 312 nm in order to determine the appropriate irradiation time. At the surface, conversion in double bonds was determined on a film applied on the ATR diamond crystal. In depth, conversion was determined on the downer side of a 5 mm thick sample directly in contact with the ATR crystal. Fig. 4 shows that HEMA double bonds conversion at the surface reaches a maximum of 87% in about 5 min. But actually, conversion in depth is not what we could expect. Indeed, taking into account the 5 mm thickness, the 312 nm irradiation wavelength, and the 6.5 mW/cm^2 incident intensity, Beer–Lambert's law predicts an intensity equal to 0.36 mW/cm^2 at the end of the 5 mm. When irradiating a film with this calculated intensity, the kinetic (Fig. 4) is quite different from that the one really observed in depth. Indeed, a 0.36 mW/cm^2 intensity generates a reaction that occurs not only later but also slower. This phenomenon of photobleaching has already been encountered elsewhere [30,31]. Indeed, the reactive mixture absorbance at 312 nm is due to the methacrylic and vinyl double bonds and also to the photoinitiator encountered in the medium. Since the photochemical reaction implies a reaction of these species, the system absorbance decreases when the irradiation takes place. Thus, the UV beam penetrates deeper and deeper as the irradiation time increases. Consequently, the medium seems to bleach during UV exposure, making the light received by the bottom increasing and becoming more intense than the calculated value. We have thus chosen irradiation time of 3 min, so that HEMA double bonds won't react in depth and will reach approximately 70% at the surface.

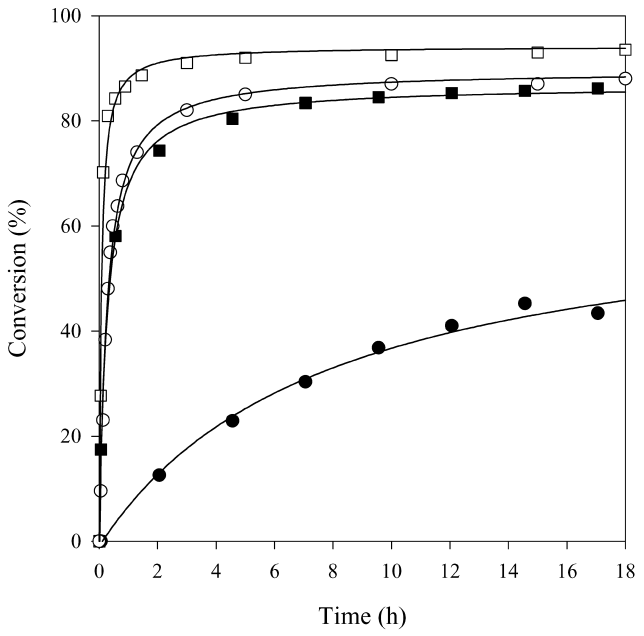

Fig. 5. Conversions of isocyanate functions, at 30 °C (■) and 80 °C (□), and HEMA double bonds at 30 °C (●) and 80 °C (○), for an unirradiated film sample versus time.

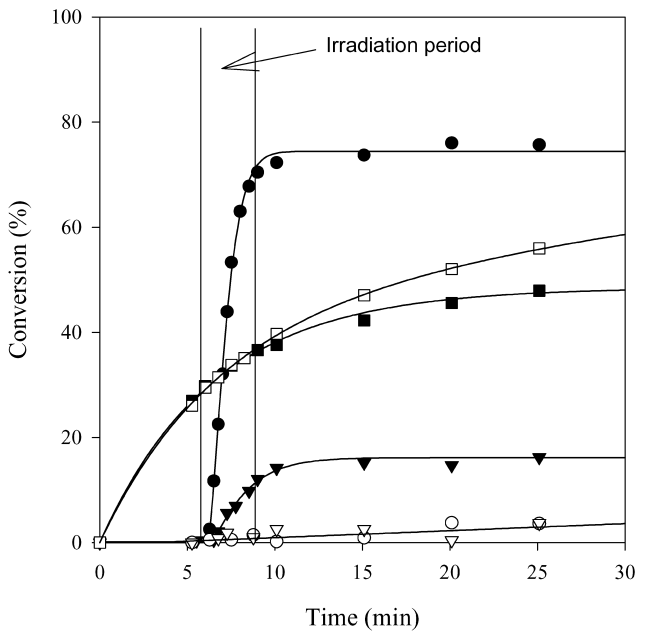

Fig. 6. Conversions of isocyanate functions at 30 °C at the surface (■) and in depth (□), HEMA double bonds at the surface (●) and in depth (○), and HTPB vinyl double bonds at the surface (▼) and in depth (▽), for a 5 mm thick sample versus time.

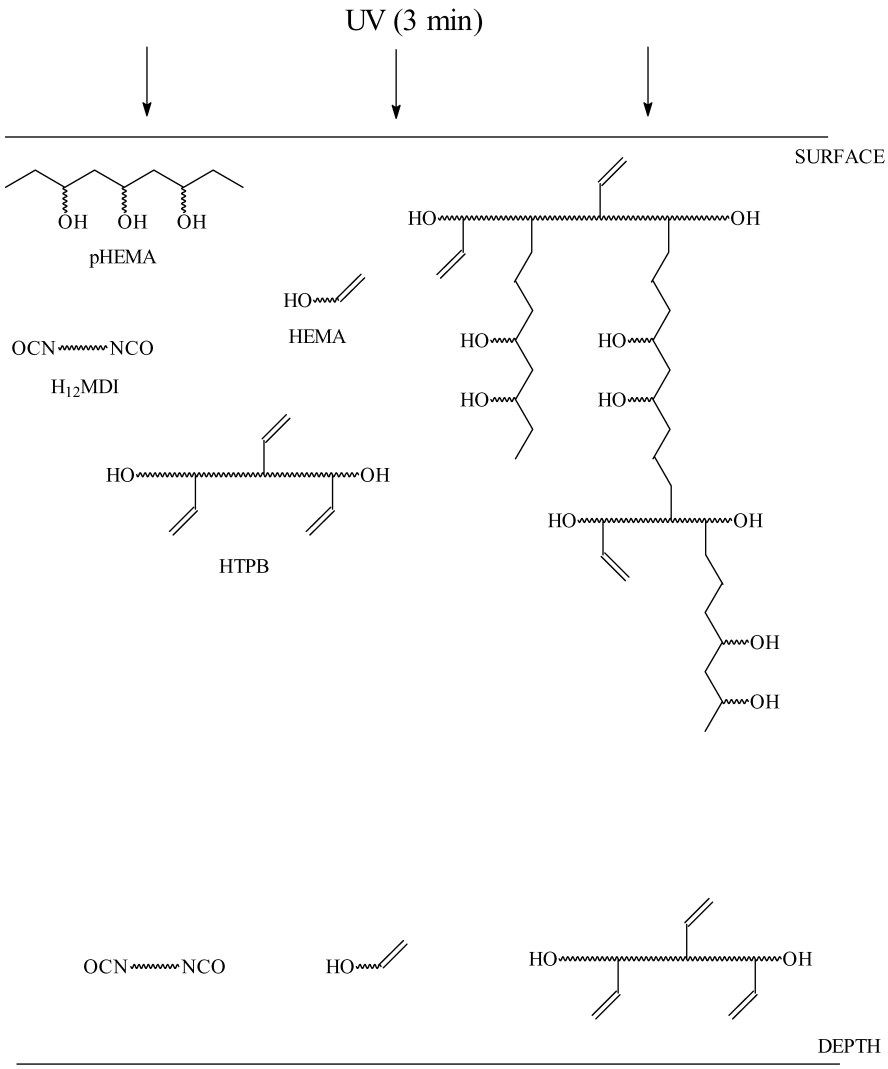

Fig. 7. Reaction scheme during photopolymerization step.

3.2. Thermal crosslinking parameters of the polyurethane network

The second step consists in crosslinking the material, in order to avoid later evolution of the gradient. This crosslinking involves H_{12}MDI which, thanks to its isocyanate functions and the hydroxyl groups of HEMA and HTPB, will react via a classical polyurethane formation reaction. A stoechiometric ratio in isocyanate functions and hydroxyl groups was chosen. The polyurethane synthesis kinetics are well-known to be sensitive to heating of the reactional medium in order to increase the kinetic, even more in bulk polymerization [32].

On the other hand, acrylate double bonds can readily react if heated. The effect of temperature on the polyurethane network formation and HEMA double bonds reaction was studied on a unirradiated film sample in Fig. 5, at 30 and 80 °C. As expected, the higher the temperature is, the faster the polyurethane formation is and the higher the ultimate conversion in isocyanate functions is, respectively, 86 and 92% at 30 and 80 °C. But the effect of temperature on HEMA double bonds is dramatic. Indeed, a 80 °C temperature leads to a fast polymerization that reaches 75% in only 2 h. This temperature is definitely not convenient. As far as the 30 °C kinetic is concerned, HEMA double bonds still react but in a slower manner. Thus, the 30 °C temperature appears to be the choice temperature to avoid, as far as possible, a too important polymerization of HEMA double bonds in depth where these functional groups are the more available.

3.3. Study of the gradient material formation

The gradient polymer is now synthesized using conditions previously mentioned. Conversions of isocyanate functions, HEMA double bonds, and HTPB vinyl double bonds at the surface and in depth are reported in Fig. 6.

Concerning HEMA double bonds, a 75% conversion at

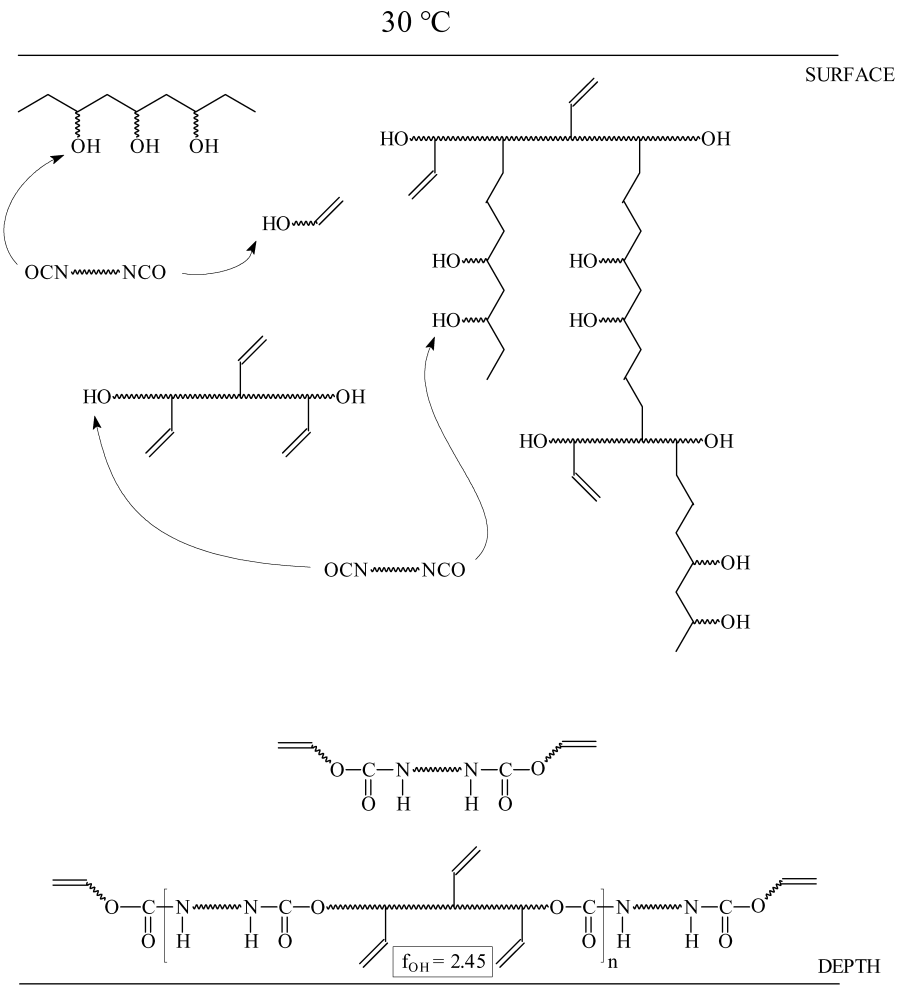

Fig. 8. Reaction scheme during thermal step.

the surface and a 5% conversion in depth can be noticed, that is to say a 70% HEMA double bonds conversion gradient. Moreover, Fig. 6 shows that HTPB vinyl double bonds react in this first step, until about 15% conversion. Therefore, we can assume that HEMA undergoes a grafting reaction towards HTPB vinyl double bonds, what was already noticed in literature [33,34]. Furthermore, it was also mentioned that polymerization of HEMA can lead to a network because of radical chain transfer mechanisms on hydroxyl groups [35–37]. Thus, as shown in Fig. 7, the UV step leads to a crosslink of the HEMA homopolymer with itself and with HTPB.

Concerning isocyanate functions, their disappearance are slower at the surface than in depth. This can be explained by the polyHEMA network created in surface that makes the diffusion of reactive species more difficult. It should be stressed that isocyanate reaction begins as soon as DBTL is introduced, in other words it takes place even during the photopolymerization step. Thus, as presented in Fig. 8, urethane functions can be created in depth between isocyanate groups of H_{12}MDI and hydroxyl groups of free HTPB and HEMA, and at the surface between isocyanate groups of H_{12}MDI and hydroxyl groups of free HTPB and HEMA and also between crosslinked HTPB and polyHEMA. Furthermore, the reaction is far from being completed after 30 min, with only a 45% conversion at the surface and 55% in depth.

Time stability of the material is studied in Fig. 9. Conversions of isocyanate functions, HEMA double bonds, and HTPB vinyl double bonds are plotted against time for the bottom of the material during 90 h. The ultimate isocyanate conversion in depth is reached in 30 h, but a strong increase of HEMA double bonds conversion is also observed.

Moreover, Fig. 10 shows a comparison of HEMA and isocyanate conversion kinetics for a 5 mm irradiated sample and an unirradiated film. The observed kinetics are very similar, i.e. HEMA reaction is only due to temperature and not to a diffusion of radicals or growing chains generated at the surface towards the bottom. This thermal polymerization of HEMA slowly occurs even at 30 °C, which leads to a 55% conversion after 4 days. Thus, we can obtain a stable gradient material after 4 days of reaction.

Finally, a 5 mm thick gradient material was cut into 0.45 mm thick layers and conversion in HEMA double bonds was measured by ATR for both sides of each layer.

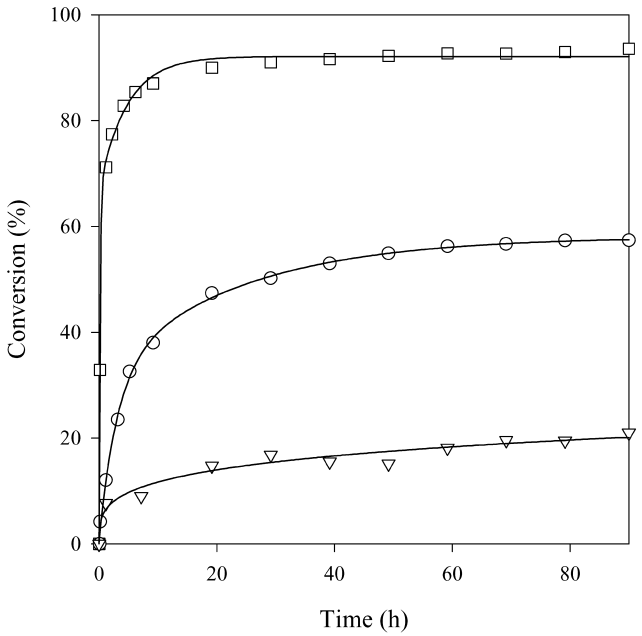

Fig. 9. Conversions of isocyanate functions (□), HEMA double bonds (○), and HTPB vinyl double bonds (▽), for a 5 mm thick irradiated sample versus time at 30 °C.

HEMA double bonds conversions plotted against thickness right after irradiation on material of variable thickness and in the ultimate material are presented in Fig. 11. We can notice that the gradient ultimately obtained is very different compared to the expected one. Indeed, the expected 70% HEMA conversion gradient has turn into a 20% gradient. In spite of this point, the ultimate material is stable through time and further irradiation doesn't affect the gradient.

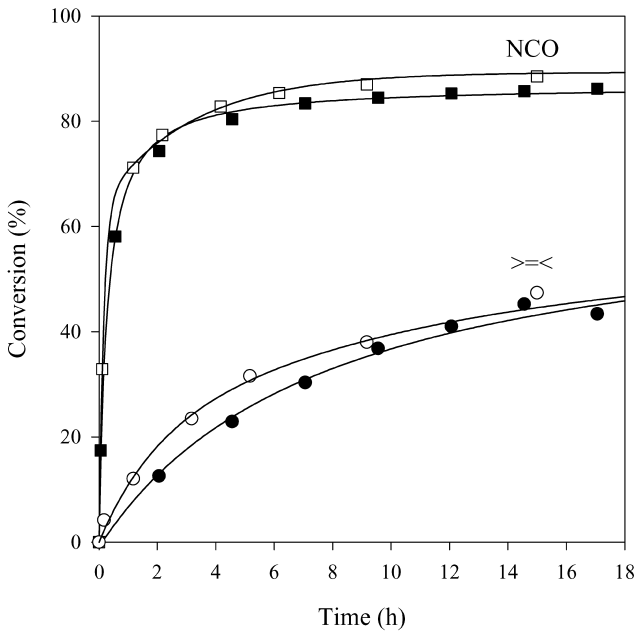

Fig. 10. Comparison of conversions of isocyanate functions and HEMA double bonds in a film without irradiation (■, ●) and in depth with irradiation (□, ○) at 30 °C.

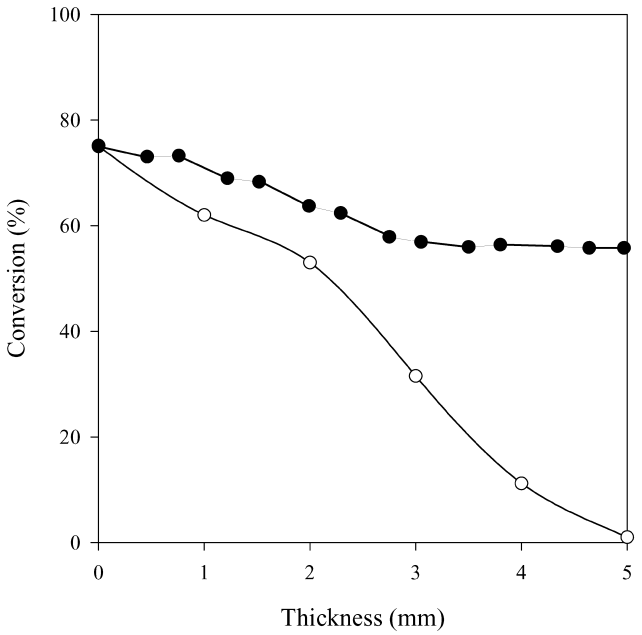

Fig. 11. Comparison of HEMA double bonds conversion right after irradiation at 30 °C on material of various thickness (○) and in both sides of the ultimate material layers (●–●).

A DMA analysis was carried out on each layer previously mentioned. The tan δ curves are shown in Fig. 12. First of all, the last three layers (layers 5–7) exhibit a very similar behaviour, which is in good agreement with their identical 55% HEMA double bonds conversion. Another important point lies in the behaviour of the layers around 120 °C. Indeed, this temperature represents the mechanical transition T_α associated with polyHEMA, and this transition decreases through the thickness and tends to

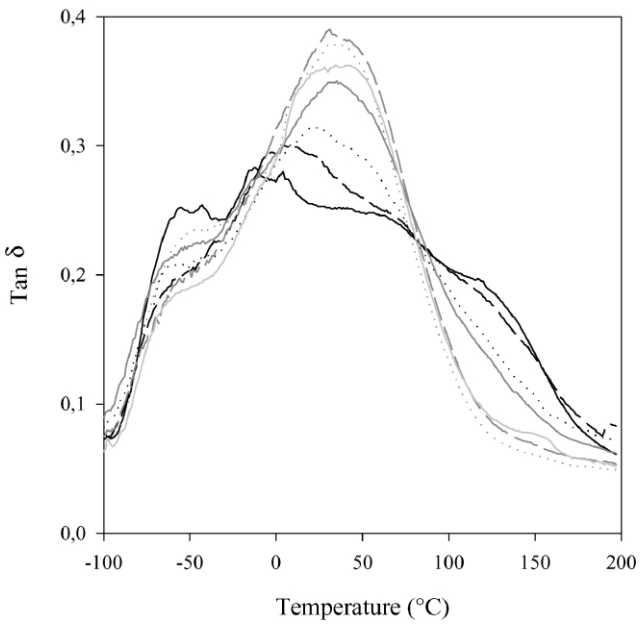

Fig. 12. Tan δ curves versus temperature for different layers (■ layer 1, – – – layer 2, ⋯ layer 3, ■ layer 4, – – – layer 5, ⋯ layer 6, ■ layer 7).

disappear in the bottom layers. As far as the other relaxations observed are concerned, the one seen around −60 °C doesn't vary significantly when thickness increases and can be assigned to HTPB soft segments. Furthermore, the mechanical analysis exhibits intermediary transitions (between −10 and 60 °C) for the top layers which evolve into a transition around 40 °C for the bottom layers. These transitions can be attributed to the different and complex crosslinked structures created during the concomitant photopolymerization and formation of polyurethane networks. Nevertheless, the bottom layers present a more narrow transition, in opposition with the broad transition of the surface. This phenomenon indicates a more homogeneous structure in depth than at the surface, as can be appreciated in Figs. 7 and 8. Although the HEMA double bonds gradient is only 20%, structures of the created networks seem to be very different at the surface and in depth.

4. Conclusion

In this study, a material presenting a polymerization gradient was successfully obtained from a homogeneous system composed of HEMA, HTPB, and H_{12}MDI using photopolymerization. The thermal crosslinking of the medium, required to set the gradient, resulted in a decrease of this gradient. Nevertheless, the ultimate gradient material obtained is stable against later UV exposure, and presents a structure gradient through the thickness due to different networks structures. The study of other reagents enabling to keep the gradient intact will be of great interest in further work.

References

[1] Milczarek P, Kryszewski M. Prog Colloid Polym Sci 1985;71:96.
[2] Milczarek P, Kryszewski M. Colloid Polym Sci 1987;265:481.
[3] Pluta M, Milczarek P, Kryszewski M. Colloid Polym Sci 1987;265:490.
[4] Xie XM, Matsuoka M, Takemura K. Polymer 1992;33:1996.
[5] Sperling L. Interpenetrating polymer networks and related materials. New York: Wiley; 1981.
[6] Lipatov Y, Sergeeva L, Karabanova L, Rosovitsky VF, Skiba SI, Babkina NV. Mech Compos Mater 1988;6:1026.
[7] Akovali G, Biliyar K, Shen M. J Appl Polym Sci 1976;20:2419.
[8] Jasso CF, Hong SD, Shen M. Am Chem Soc Adv Chem Ser Multiphase Polym 1979;23:444.
[9] Martin GC, Enssani E, Shen M. J Appl Polym Sci 1981;26:1465.
[10] Shen M, Bever MB. J Mater Sci 1972;7:741.
[11] Dror M, Elsabee MZ, Berry GC. J Appl Polym Sci 1981;26:1741.
[12] Mueller KF, Heiber SJ. J Appl Polym Sci 1982;27:4043.
[13] Koike Y, Tanio N, Nihei E, Ohtsuka Y. Polym Engng Sci 1989;29:1200.
[14] Wang DJ, Gu CB, Chen PL, Liu SX, Zhen Z, Zhang JC, Liu XH. J Appl Polym Sci 2003;87(2):280.
[15] Agari Y, Shimada M, Ueda A, Nagai S. Macromol Chem Phys 1996;197:2017.
[16] Murayama S, Kuroda S, Osawa W. Polymer 1993;34(18):3893.
[17] Karabanova LV, Sergeeva LM, Lutsyk ED, Kuznetsova VP. Polym Sci Ser A 1996;38(10):1108.
[18] Jasso CF, Martinez JJ, Mendizabal E, Laguna O. J Appl Polym Sci 1995;58:2207.
[19] Karabanova L, Pissis P, Kanapitsas A, Lutsyk E. J Appl Polym Sci 1998;68:161.
[20] Akovali G. J Appl Polym Sci 1999;73:1721.
[21] Sorm M. La Technique Moderne 1988;19. (7–8):19.
[22] Ohtsuka Y. Appl Phys Lett 1973;23(5):247.
[23] Dror M, Elsabee MZ, Berry GC. Biomater Med Dev Art Org 1979;7(1):31.
[24] Beauregard GP, James SP. Biomed Sci Instrum 1999;35:415.
[25] Lipatov YS, Karabanova LV, Gorbach LA, Lutsyk ED, Sergeeva LM. Polym Int 1992;28:99.
[26] Elsabee MZ, Dror M, Berry GC. J Appl Polym Sci 1983;28:2151.
[27] Jasso CF, Valdéz J, Pérez JH, Laguna O. J Appl Polym Sci 2001;80:1343.
[28] Lipatov YS, Karabanova LV. J Mater Sci 1995;30:1095.
[29] Poletto S, Pham QT. Macromol Chem Phys 1994;195:3901.
[30] Rutsch W, Dietliker K, Leppard D, Kölher M, Misev L, Kolczak U, Rist G. Prog Org Coat 1996;27:227.
[31] Miller GA, Gou L, Narayanan V, Scranton AB. J Polym Sci Part A 2002;40(6):793.
[32] Grigor'eva VA, Baturin SM, Entelis SG. Vysokomol Soedin Ser A 1972;14:1345.
[33] Huang NJ, Sundberg DC. J Polym Sci Part A 1995;33:2587.
[34] Mateo JL, Calvo M, Bosch P. J Polym Sci Part A 2001;39:2444.
[35] Gregonis DE, Russell GS, Andrade JD, de Visser AC. Polymer 1978;19:1279.
[36] Montheard JP, Chatzopoulos M, Chappard D. J Macromol Sci—Rev Macromol Chem Phys 1992;C32(1):1.
[37] Morra M, Occhiello E, Garbassi FJ. J Colloid Interf Sci 1992;149:84.